

Impact of Next-Nearest-Neighbor hopping on Ferromagnetism in GaMnN

Sourav Chakraborty¹, Subrat K Das², Kalpataru Pradhan¹

¹*CMP Division, Saha Institute of Nuclear Physics, HBNI, Kolkata 700064, India*

²*SKCG Autonomous College, Paralakhemundi, Odisha 761200, India*

Being a wide band gap system GaMnN attracted considerable interest after the discovery of highest reported ferromagnetic transition temperature $T_C \sim 940$ K among all diluted magnetic semiconductors. Later it become a debate due to the observation of either a ferromagnetic state with very low $T_C \sim 8$ K or sometimes no ferromagnetic state at all. We address these issues by calculating the ferromagnetic window, T_C Vs p , within a $t-t'$ Kondo lattice model using a spin-fermion Monte-Carlo method on a simple cubic lattice. We exploit the next-nearest-neighbor hopping t' to tune the degree of delocalization of the free carriers and show that carrier localization (delocalization) significantly widen (shrunk) the ferromagnetic window with a reduction (enhancement) of the optimum T_C . We connect our results with the experimental findings and try to understand the ambiguities in ferromagnetism in GaMnN.

Search for high T_C ferromagnetism in diluted magnetic semiconductors (DMSs) has been a topic of core importance over last two decades in view of potential technological applications¹⁻⁴. Mn doped GaAs (GaMnAs)⁵⁻¹⁰ is one of the most extensively investigated DMS with highest reported $T_C \sim 200$ K¹¹, which is well below the room temperature. In the mean time, wide band gap based DMS had attracted considerable interest after the discovery of room temperature T_C in Mn doped GaN (GaMnN)^{12,13}, but soon realized that getting a ferromagnetic state in GaMnN is often challenging¹⁴. The nature of ferromagnetism in this material is poorly understood as compared to GaMnAs, and so uncertainty in getting a ferromagnetic state is still a debated question^{14,15}.

The nature of ferromagnetism in GaMnAs reasonably well understood^{3,4}, and so regarded as the benchmark to understand other similar DMSs. Here, a few percentage of Mn^{2+} ion ($S = 5/2$) replaces Ga^{3+} , thereby contributes a hole which mediate the magnetic interaction between the Mn spins. But the hole density (holes per Mn ions) is smaller than 1 due to As antisites¹⁶ (As_{Ga}) and Mn interstitials¹⁷ (Mn_{I}) which act as double donors. It is well known that post-growth annealing is an effective technique to alter the hole density¹⁸. These holes reside in the shallow acceptor level introduced by Mn ions in the host band gap ~ 0.1 eV above the valence band¹⁹⁻²², which indicates the long-range nature of magnetic interactions between the Mn ions. With increasing impurity concentration x these levels form a distinct spin-polarized impurity band (IB). Now, it is known that the location of the Fermi energy E_F within the IB plays a crucial role in determining the T_C ²³. Also, the ferromagnetic window is reported for a wide range of hole density ($p \sim 0.1-0.9$)^{23,24}. But a significant limitation of GaMnAs is that the ferromagnetic T_C is well below the room temperature.

Wide band gap semiconductors^{9,14} had attracted immense interest after the reports^{12,13} of ferromagnetic T_C over 300 K in GaMnN. However, the physical origin of the ferromagnetism in this material still remains controversial as some authors observed a very low $T_C \sim 8$ K or did not see any ferromagnetism at all²⁵. In contrast

to GaMnAs, Mn is deep acceptor in GaMnN forming a distinct narrow impurity band that is ~ 1.5 eV^{21,26-31} above the valence band maximum. Consequently, the hole mediated interactions between the Mn ions are short range in nature. Where, p-type co-doping (with Mg in the case of GaMnN) has shown to enhance the carrier mediated ferromagnetism³², the theoretical studies found that extrinsic doping of p-type generating defects such as Gallium vacancies reduce the stability of the ferromagnetic state³³. In addition, the coexistence of Mn^{2+} (majority) and Mn^{3+} (minority)³⁴ and the nature of defect states³³⁻³⁵ have made the nature of ferromagnetism in GaMnN more complicated compared to GaMnAs. So, the theoretical studies to understand the ferromagnetism in GaMnN remains inconclusive till date.

Aim of this paper is to shed light on the unresolved aspects of GaMnN where the high ferromagnetic T_C remains illusive till date. We consider a $t-t'$ Kondo lattice model and calculate the magnetic and the transport properties using a traveling cluster approximation based spin-fermion Monte-Carlo method³⁶ on a simple cubic lattice. Degree of delocalization of the free carriers and hence the magnetic properties are exploited by tuning the next-nearest-neighbor hopping t' . We start with a brief introduction to the model Hamiltonian and the methodology of our calculations. After that organization of this paper is threefold: first, we establish appropriate set of parameter for GaMnAs and GaMnN. In the second part we investigate the electronic and magnetic properties of Mn-doped GaAs system and finally we calculate and discuss our results for GaMnN.

We consider the diluted Kondo lattice Hamiltonian³⁷⁻⁴⁰

$$H = -t \sum_{\langle ij \rangle \sigma} c_{i\sigma}^\dagger c_{j\sigma} - t' \sum_{\langle\langle ij \rangle\rangle \sigma} c_{i\sigma}^\dagger c_{j\sigma} + J_H \sum_m \mathbf{S}_m \cdot \vec{\sigma}_m$$

on a simple cubic lattice, where $c_{i\sigma}^\dagger$ ($c_{i\sigma}$) are the fermion creation (annihilation) operators at site i with spin σ . t and t' are the nearest-neighbor ($\langle ij \rangle$) and the NNN hopping parameters ($\langle\langle i,j \rangle\rangle$), respectively. The last term

represents the Hund's coupling J_H (> 0) between the impurity spin \mathbf{S}_m and the itinerant electrons $\bar{\sigma}_m$, represented by Pauli spin matrices, at randomly chosen site m . We considered the spin S_m to be classical and absorb its magnitude $5/2$ into J_H without loss of generality. Direct exchange interaction between the localized spins due to magnetic moment clustering is neglected by avoiding the nearest neighbor Mn pairing. For impurity concentration x we have $x10^3$ number of spins and the carrier density p is defined as the holes per Mn impurity site. We consider $x = 0.15-0.25$ in the simple cubic lattice, where as GaAs is face centered cubic with four atoms per unit cell. So, roughly 25% of x in our case corresponds to 6.25% that in real experiments. We chose $t = 0.5$ eV by comparing the bare bandwidth ($= 12t$) of our model to that of the realistic bandwidth 6 eV for the host III-V semiconductors. Parameters like J_H , t' , and temperature T are scaled with t .

The model Hamiltonian incorporating spatial fluctuations due to randomly distributed magnetic impurities, as in DMSs, must be carried out for a reasonably large system size for better results of the physical quantities such as T_C ^{37,40}. We use the exact diagonalization based classical Monte-Carlo method to anneal the system towards the ground state at fixed carrier density and temperature. First, the classical spin \mathbf{S}_m is updated at a site and in this background of new spin configuration the internal energy is calculated by exact diagonalization of the carriers. Then, the proposed update is accepted or rejected by using the Metropolis algorithm. A single system sweep composed of the above processes repeated over each classical spin once. Note, the exact diagonalization grows as $\mathcal{O}(N^4)$ per system sweep and numerically too expensive for a system size of $N = 10^3$, where at each temperature we require at least over 1000 system sweeps to anneal the system properly. We avoid the size limitation by employing a Monte-Carlo technique based on travelling cluster approximation (TCA)^{36,41} in which computational cost drops to $\mathcal{O}(N \times N_c^3)$ for each system sweep. Here, N_c is size of the moving cluster reconstructed around the to-be-updated site and the corresponding Hamiltonian is diagonalized rather than that of the full lattice. This allows us to handle a system size of $N = 10^3$ using a moving cluster of size $N_c = 6^3$. All physical quantities are averaged over several different such random configurations of magnetic impurities.

The nature of the impurity band plays the key role in determining the ferromagnetic state which solely depends on the exchange interaction J_H and the amount of the magnetic impurities x in the system. Ultra-fast transient reflectivity spectra⁴² and magnetic circular dichroism measurements²³ show the existence of a preformed impurity band close to the valence band (VB) in GaMnAs. We start our calculation for $x = 0.25$, where a separated impurity band (IB) starts to form for $J_H = 4$ (even at relatively high temperature $T = 0.05$) as shown in the density of states (DOS) $N(\omega) = \langle \frac{1}{N} \sum_{\alpha} \delta(\omega - \epsilon_{\alpha}) \rangle$ in Fig. 1(a). Here, the binding energy E_b (= bottom of

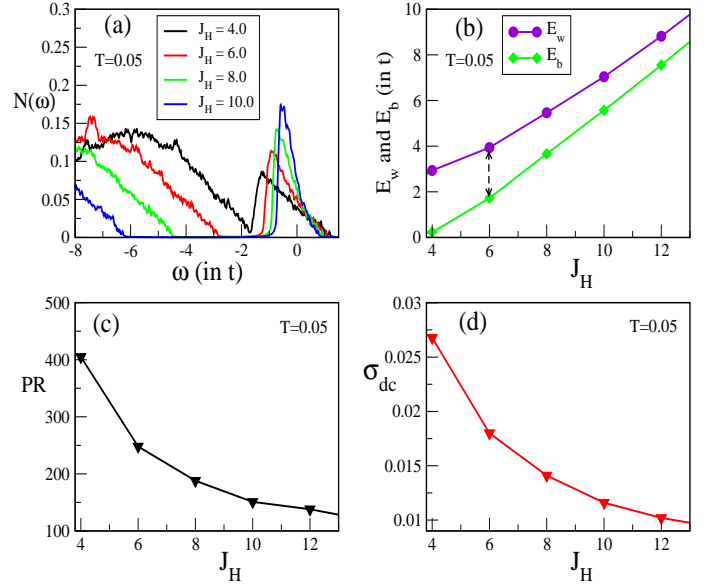


FIG. 1: (a) Shows the density of states $N(\omega)$ with the formation of impurity band for different values of the Hund's coupling J_H . Fermi energy is set at zero; (b) variation of the binding energy E_b and the E_w with J_H showing the localization-induced narrowing of the impurity band; (c) variation of the participation ratio with J_H distinguishing the extended states from the localized states; (d) plots the dc conductivity (in units of $\pi e^2 / h a$) with J_H indicating carrier localization as in (c). All calculations are done at fixed impurity concentration $x = 0.25$, carrier concentration $p = 0.2$, and temperature $T = 0.05$.

the IB - top of the VB) is $\sim 0.2t$, where the small finite density of states at the Fermi energy is due to the broadening used to calculate the DOS. We define the quantity E_w = top of the IB - top of the VB, which must be smaller than the band gap of the host semiconductor. With increasing J_H the IB moves away from the VB and also its width ($E_w - E_b$) becomes narrow, which indicate the increase in carrier localization with J_H [Fig. 1(b)].

The solubility of Mn in GaAs and GaN is low and it is well known that the semiconducting property of the host materials remain intact after the introduction of the magnetic impurities. The band gap of GaMnN is ~ 3.4 eV. The impurity band is distinctly separated from the valence band located at an energy ~ 1.5 eV (E_b) above the VB indicating the short-range nature of the ferromagnetic interactions. In contrast, GaMnAs is a low band gap (~ 1.5 eV) system with long-ranged ferromagnetic interaction where the E_b is only about ~ 0.1 eV. So, we choose $J_H = 4$ for GaMnAs for which $E_b \sim 0.1$ eV ($0.2t$) and E_w is ~ 1.5 eV ($3t$). Direct measurements yield $J_H = 1.2$ eV [7,8] and 3.3 eV [6] for GaMnAs. Note that we absorbed the impurity spin magnitude $5/2$ into J_H which scales with t ($= 0.5$ eV). So our J_H value is in the range as reported in experiments. In case of GaMnN we chose $J_H = 10$, where $E_b \sim 2.75$ eV and E_w is ~ 3.5 eV ($7t$). Later, we will see the impact of NNN hopping t' on

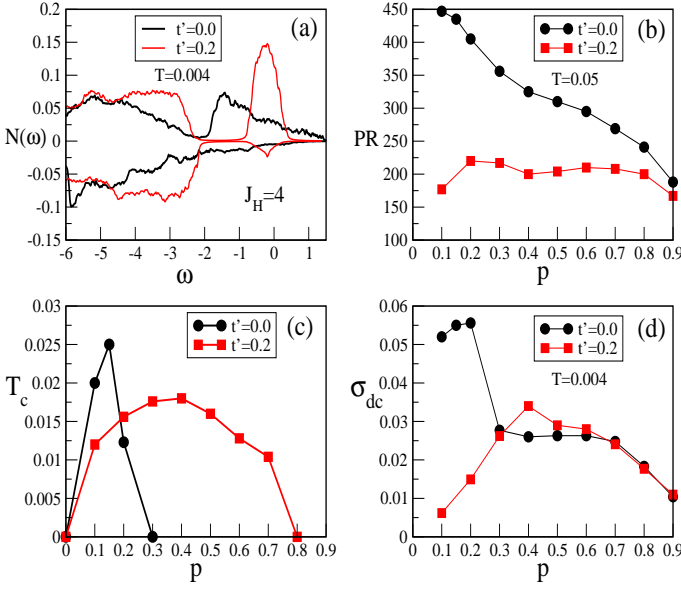


FIG. 2: The effects of the next-nearest-neighbor hopping ($t' = +0.2$) and its comparison to $t' = 0$ is shown for various physical quantities at fixed $J_H = 4$. (a) Plots the spin-resolved density of states at fixed $T = 0.004$, where the impurity band shrinks and moves away from the valence band due to carrier localization. The Fermi energy is set at zero; (b) change in the participation ratio with p showing the higher degree of localization for $t' = +0.2$ at fixed $T = 0.05$; (c) showing the t' -induced broadening of the ferromagnetic window T_c Vs p and (d) plots the dc conductivities (in units of $\pi e^2/h\alpha$) with p at fixed $T = 0.004$. The localization driven I-M-I transition is consistent with the results presented in (b) and (c).

the IB and its consequence on the ferromagnetic state.

The degree of delocalization can be inferred from the participation ratio (PR), which ranges from 1 to the total number of sites N and allows us to distinguish the localized states (low PR) from the fully extended states ($PR \sim N$). We plot the PR of the state at the Fermi energy (E_F) with J_H for $p = 0.2$ at $T = 0.05$ [Fig. 1(c)]. For the chosen Hund's couplings $J_H = 4$ and 10 the states are extended over ~ 400 sites and only over ~ 150 sites respectively, which indicate that the short- and long-range nature of the exchange interactions in GaMnAs and GaMnN are automatically taken into account. Then we calculate the dc limit of the conductivity by using the Kubo-Greenwood formula^{43,44} for fixed $p = 0.2$ at $T = 0.05$ and shown in Fig. 1(d). The conductivity decreases with J_H values, which substantiate the fact that the carriers get localized with Hund's coupling as seen in Fig. 1(c). Next, we study the impact of NNN hopping on the magnetic properties in GaMnAs and in GaMnN.

First, we study the GaMnAs with the chosen Hund's coupling $J_H = 4$. Fig. 2(a) presents the spin-resolved density of states for $t'=0$ and 0.2 with fixed $p=0.2$ at $T = 0.004$ for which ground states are ferromagnetic. In both cases the impurity band is spin polarized while the valence band remains more or less unpolarized. In our

model +ve t' acts as a localizing agent which can be visualized from the DOS, where the IB becomes narrow and shifts away from the VB. This is also apparently clear from the PR plotted in Fig. 2(b). It is important to note that here t' doesn't alter the value of E_w ($\sim 3t$) which is well within the BG of the host. Alternatively, higher J_H can also localize the carriers but E_w becomes larger than the BG which is not physically acceptable for narrow BG host semiconductors like GaAs, we will see later.

Then we plot the ferromagnetic T_C with the carrier density p in Fig. 2(c). The ferromagnetic T_C is estimated from the ferromagnetic structure factor $S(\mathbf{0})$, where $S(\mathbf{q}) = \frac{1}{N} \sum_{ij} \mathbf{S}_i \cdot \mathbf{S}_j e^{i\mathbf{q} \cdot (\mathbf{r}_i - \mathbf{r}_j)}$ for each carrier density. For $t'=0$ the T_C optimizes around $p=0.15$ and the ferromagnetism is restricted to a small window of $p = 0-0.3$. This is because the carrier mobility is suppressed at higher hole concentration (0.3 or more) due to larger delocalization length in this case, see Fig. 1(c). One can demobilize the carriers and hence activate the ferromagnetism at higher p values with mildly localizing the carriers which is done by the NNN hopping parameter $t' = 0.2$ as shown in Fig. 2(b). Consequently, the ferromagnetic window becomes wider ($p = 0-0.8$) as observed in the experiments [$p \sim 0.1-0.9$]^{23,24}. In order to correlate the magnetic and transport properties we plot the the low temperature ($T = 0.004$) dc conductivity in Fig. 2(d). For both $t' = 0$ and 0.2 , conductivity goes through Insulator-Metal-Insulator (I-M-I) transition with optimization around the same value of p as in case of T_C vs p window which supports the above carrier localization picture. Our results on the FM window indicate that the NNN is operative in real systems and must be taken in to account in theoretical investigations.

Now, we consider the GaMnN where the magnetic interactions is driven by the double-exchange mechanism with short-range spin-spin interactions. Hence, we chose the Hund's coupling $J_H = 10$ consistent with the the E_w and E_b values of the system as mentioned earlier. The spin-resolved DOS for $t' = 0$ and 0.2 with fixed $p = 0.2$ at $T = 0.004$ are shown in Fig. 3(a). Effect of NNN hopping on IB is qualitatively similar as in Fig. 2(a) with E_w within the BG of the host. Effects of t' on the ferromagnetic state is presented in Fig. 3(b). Besides the widening of the FM window, the optimum value of T_C significantly decreases as compared to $t' = 0$ case. The reduction in the optimum T_C is due to the localization, which can be visualized from the nature of the IBs shown in Fig. 3(a). T_C can be tuned further by adjusting the t' value. These results guide us to understand the very low T_C often reported in GaMnN.

The electronic structure calculations show that the Ga defects introduce states between the VB and the IB which depopulate the IB and in turn destroy the ferromagnetism in GaMnN³³. We mimic the situation by introducing -ve NNN hopping which delocalize the carriers and consequently broaden the IB towards the VB. This can be seen from the DOS plotted in Fig. 3(c) for $t' = -0.2$ and -0.5 along with $t' = 0$ at $T = 0.004$ and $p = 0.2$.

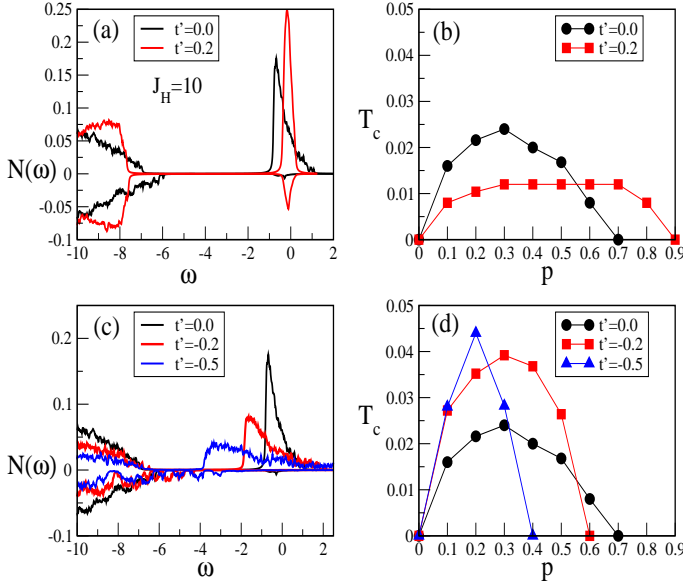


FIG. 3: The effects of the localized hopping $t' = +0.2$ and its comparison to $t' = 0$ are presented for (a) the spin-resolved density of states at fixed $T = 0.004$, where the impurity band moves away from the valence band due to carrier localization; (b) the ferromagnetic window T_C Vs p showing the localization-induced broadening. And, the effects of the delocalized hopping $t' = -0.2$ and -0.5 with its comparison to $t' = 0$ are presented for (c) the spin-resolved density of states at fixed $T = 0.004$, where the impurity band extended towards the valence band due to carrier delocalization, and (d) the ferromagnetic windows showing the delocalization-induced shrinking. The Fermi energy is set at zero and $J_H = 10$ for all calculations.

Here, the binding energy E_b decreases but E_w remains unaffected (i.e. E_w is within the BG). Consequently, the ferromagnetic window shrinks and the T_C increases with carrier delocalization, which can be understood from the analysis given in Fig. 2(c) and Fig. 3(b). Next, we see the impact of the t' -induced delocalization on the ferromagnetism in the lower impurity concentration regime.

It is clear from Fig. 3(c) that the width of IB increases and as a result DOS depopulates at Fermi levels for NNN $t' = -0.2$ and $t' = -0.5$. This depopulation destabilizes the ferromagnetic interaction at higher p values. We establish our findings by calculating the ferromagnetic windows for lower values of $x = 0.15$ and 0.2 . First we consider $x = 0.2$, and compare the spin-resolved DOS and the ferromagnetic windows for different values of t' ($= 0.0, -0.2$, and -0.5) at fixed $p = 0.2$, as shown in Fig. 4(a) and (b) respectively. Similar set of calculations are presented in Fig. 4(c) and (d) for $x = 0.15$ with the same set of parameters. In both cases the IB shows qualitatively similar features as in $x = 0.25$ [see Fig. 3(c)]. As compared to the case of $x = 0.25$ the FM window in lower x systems are more sensitive to the NNN hopping and become significantly narrow, which reduces the probability of getting a FM state unless the sample has

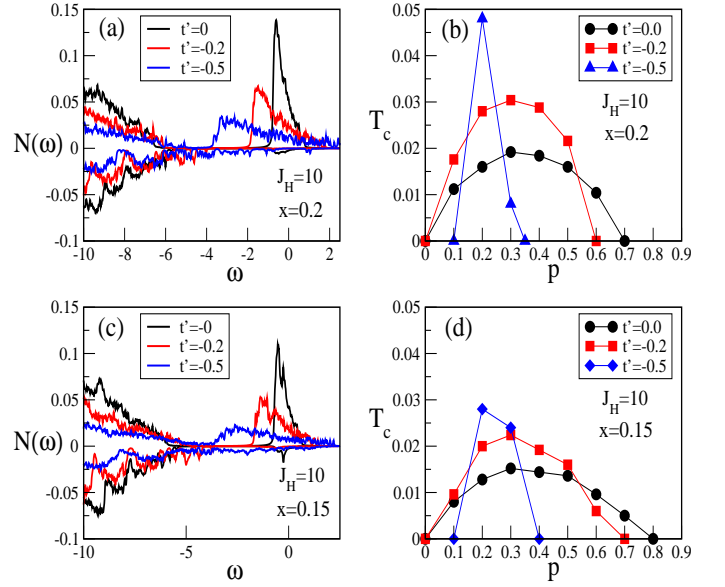


FIG. 4: The effects of the delocalized hopping $t' = -0.2$ and -0.5 with its comparison to $t' = 0$ at fixed $x = 0.2$ are shown for (a) the spin-resolved density of states at fixed $T = 0.004$ and (b) the ferromagnetic windows T_C Vs p . Similar set of calculations for $x = 0.15$ are presented in (c) and (d), respectively. Comparing to $x = 0.25$ the FM window in lower x systems are more sensitive to delocalization and becomes significantly narrow. We fixed $J_H = 10$ for all calculations.

suitable amount of carriers within a narrow regime. In experiments sample preparation is very crucial due to the presence of defects and our results indicate that if one doesn't hit a suitable combination of x and p , then there is a higher chance to observe either low T_C or no ferromagnetism at all.

In conclusion, we investigate the III-V DMSs within a $t - t'$ Kondo lattice model and calculate the magnetic and the transport properties using a classical Monte-Carlo method on a simple cubic lattice. We have shown that the carrier localization/delocalization induced by the NNN hopping t' plays a key role in determining the ferromagnetic states of GaMnAs and GaMnN. In case of GaMnAs a weak localization (small +ve t') is necessary to reproduce the robustness of the ferromagnetic states as observed in experiments. In addition, its presence seems to be necessary in describing the low T_C ferromagnetism often reported in GaMnN. On the other hand, if we delocalize the carriers by activating -ve t' the ferromagnetic window significantly shrinks with an enhancement of the optimum value of T_C in GaMnN. We correlate our findings with the experimental results and suggest that Ga vacancy in GaMnN that depopulate the IB triggers high T_C in low hole density. But in reality, the presence of intrinsic defects is inevitable and also the carrier density is not controllable. So the probability of having an optimal amount of holes in a narrow regime in Ga defected GaMnN is very low. This could be the reason of disap-

pearance of ferromagnetism and in turn keeps the high T_C issue of GaMnN unresolved till date.

Acknowledgment: We acknowledge use of Meghnad2019 computer cluster at SINP.

KP: kalpataru.pradhan@saha.ac.in

SKD: skdiitk@gmail.com (Present Address: Plot No-151, R & R Colony, Shillong, Meghalaya, India)

- ¹ H. Munekata, H. Ohno, S. von Molnar, Armin Segmueller, L. L. Chang, and L. Esaki, Phys. Rev. Lett. **63**, 1849 (1989).
- ² H. Ohno, Science **281**, 951 (1998).
- ³ T. Jungwirth, Jairo Sinova, J. Masek, J. Kucera, and A. H. MacDonald, Rev. Mod. Phys. **78**, 809 (2006).
- ⁴ T. Dietl and H. Ohno, Rev. Mod. Phys. **86**, 187 (2014).
- ⁵ H. Ohno, A. Shen, F. Matsukura, A. Oiwa, A. Endo, S. Katsumoto, and Y. Iye, Appl. Phys. Lett. **69**, 363 (1996).
- ⁶ F. Matsukura, H. Ohno, A. Shen, and Y. Sugawara, Phys. Rev. B **57**, R2037(R) (1998).
- ⁷ J. Okabayashi, A. Kimura, O. Rader, T. Mizokawa, A. Fujimori, T. Hayashi, and M. Tanaka, Phys. Rev. B **58**, R4211(R) (1998).
- ⁸ K. Ando, T. Hayashi, M. Tanaka, and A. Twardowski, J. Appl. Phys. **83**, 6548 (1998).
- ⁹ T. Dietl, H. Ohno, F. Matsukura, J. Cibert, and D. Ferrand, Science **287**, 1019 (2000).
- ¹⁰ T. Jungwirth, K. Y. Wang, J. Masek, K. W. Edmonds, Juergen Koenig, Jairo Sinova, M. Polini, N. A. Goncharuk, A. H. MacDonald, M. Sawicki, A. W. Rushforth, R. P. Campion, L. X. Zhao, C. T. Foxon, and B. L. Gallagher, Phys. Rev. B **72**, 165204 (2005).
- ¹¹ L. Chen, X. Yang, F. Yang, J. Zhao, J. Misuraca, P. Xiong, and S. von Molnar, Nano Lett. **11**, 2584 (2011).
- ¹² S. Sonoda, S. Shimizu, T. Sasaki, Y. Yamamoto, and H. Hori, J. Cryst. Growth **1358**, 237 (2002).
- ¹³ M. L. Reed, N. A. El-Masry, H. H. Stadelmaier, M. K. Ritums, M. J. Reed, C. A. Parker, J. C. Roberts, and S. M. Bedair, Appl. Phys. Lett. **79**, 3473 (2001).
- ¹⁴ K. Sato et al. Rev. Mod. Phys. **82**, 1633 (2010).
- ¹⁵ T. Dietl, Nat. Mat. **9**, 965 (2010).
- ¹⁶ R. C. Myers, B. L. Sheu, A. W. Jackson, A. C. Gossard, P. Schiffer, N. Samarth, and D. D. Awschalom, Phys. Rev. B **74**, 155203 (2006).
- ¹⁷ K. M. Yu, W. Walukiewicz, T. Wojtowicz, I. Kuryliszyn, X. Liu, Y. Sasaki, and J. K. Furdyna, Phys. Rev. B **65**, 201303(R) (2002).
- ¹⁸ S. Potashnik, K. C. Ku, S. H. Chun, J. J. Berry, N. Samarth, and P. Schiffer, Appl. Phys. Lett. **79**, 1495 (2001).
- ¹⁹ J. Szczytko, W. Mac, A. Twardowski, F. Matsukura, and H. Ohno, Phys. Rev. B **59**, 12, 935 (1999).
- ²⁰ Manish Jain, Leeor Kronik, and James R. Chelikowsky, Vitaliy V. Godlevsky, Phys. Rev. B **64**, 245205 (2001).
- ²¹ M. Wierzbowska, D. Sanchez-Portal, and S. Sanvito Phys. Rev. B **70**, 235209 (2004).
- ²² B. Sanyal, O. Bengone, and S. Mirbt, Phys. Rev. B **68**, 205210 (2003).
- ²³ M. Dobrowolska, K. Tivakornsasithorn, X. Liu, J. K. Furdyna, M. Berciu, K. M. Yu, and W. Walukiewicz, Nat. Mat. **11**, 444 (2012).
- ²⁴ Y. J. Cho, K. M. Yu, X. Liu, W. Walukiewicz, and J. K. Furdyna, Appl. Phys. Lett. **93**, 262505 (2008).
- ²⁵ E. Sarigiannidou, F. Wilhelm, E. Monroy, R. M. Galera, E. Bellet-Amalric, A. Rogalev, J. Goulon, J. Cibert, and H. Mariette, Phys. Rev. B **74**, 041306R (2006).
- ²⁶ P. Mahadevan and A. Zunger, Appl. Phys. Lett. **85**, 2860 (2004).
- ²⁷ T. Graf, M. Gjukic, M. S. Brandt, M. Stutzmann, and O. Ambacher, Appl. Phys. Lett. **81**, 5159 (2002).
- ²⁸ L. Janicki, G. Kunert, M. Sawicki, E. Piskorska-Hommel, K. Gas, R. Jakiela, D. Hommel, and R. Kudrawiec, Scientific Reports **7**, 41877 (2017).
- ²⁹ Leeor Kronik, Manish Jain, and James R. Chelikowsky, Phys. Rev. B **66**, 041203R (2002).
- ³⁰ R. Bouzerar and G. Bouzerar, Europhys. Lett. **92**, 47006 (2010).
- ³¹ R.Y. Korotkov, J. M. Gregie, and B. W. Wessels, Appl. Phys. Lett. **80**, 1731 (2002).
- ³² K. H. Kim, K. J. Lee, D. J. Kim, H. J. Kim, and Y. E. Ihm, C. G. Kim, S. H. Yoo and C. S. Kim, Appl. Phys. Lett. **82**, 4755 (2003).
- ³³ Priya Mahadevan and S. Mahalakshmi, Phys. Rev. B **73**, 153201 (2006).
- ³⁴ S. Sonoda, I. Tanaka, H. Ikeno, T. Yamamoto, F. Oba, T. Araki, Y. Yamamoto, K. Suga, Y. Nanishi, Y. Akasaka, K. Kindo and H. Hori, J. Phys.: Condens. Matter **18**, 4615 (2006).
- ³⁵ S. Limpijumnong and C. G. Van de Walle, Phys. Rev. B **69**, 035207 (2004).
- ³⁶ S. Kumar and P. Majumdar, Eur. Phys. J. B **50**, 571 (2006).
- ³⁷ G. Alvarez, M. Mayr, and E. Dagotto, Phys. Rev. Lett. **89**, 277202 (2002).
- ³⁸ A. Chattopadhyay, S. Das Sarma, and A. J. Millis, Phys. Rev. Lett. **87**, 227202 (2001).
- ³⁹ Mona Berciu and R. N. Bhatt, Phys. Rev. Lett. **87**, 107203 (2001).
- ⁴⁰ K. Pradhan and P. Majumdar, Euro. Phys. Lett. **85**, 37007 (2009).
- ⁴¹ K. Pradhan and S. K. Das, Scientific Reports **7**, 9603 (2017).
- ⁴² T. Ishii, T. Kawazoe, Y. Hashimoto, H. Terada, I. Muneta, M. Ohtsu, M. Tanaka, and S. Ohya, Phys. Rev. B **93**, 241303R (2016).
- ⁴³ G. D. Mahan, *Quantum Many Particle Physics* (Plenum Press, New York, 1990).
- ⁴⁴ S. Kumar and P. Majumdar, Europhys. Lett. **65**, 75 (2004).